The EBP50-moesin interaction involves a binding site regulated by direct masking on the FERM domain

Casey M. Finnerty[1], David Chambers[1], Janet Ingraffea[1], H. Richard Faber[2], P. Andrew Karplus[2] and Anthony Bretscher[1,*]

[1]Department of Molecular Biology and Genetics, Biotechnology Building, Cornell University, Ithaca, NY14853, USA
[2]Department of Biochemistry and Biophysics, Oregon State University, Corvallis, OR 97331, USA
*Author for correspondence (e-mail: apb5@cornell.edu)

Accepted 25 November 2003
Journal of Cell Science 117, 1547-1552 Published by The Company of Biologists 2004
doi:10.1242/jcs.01038

Summary

Members of the ezrin-radixin-moesin (ERM) protein family serve as regulated microfilament-membrane crosslinking proteins that, upon activation, bind the scaffolding protein ERM-phosphoprotein of 50 kDa (EBP50). Here we report a 3.5 Å resolution diffraction analysis of a complex between the active moesin N-terminal FERM domain and a 38 residue peptide from the C terminus of EBP50. This crystallographic result, combined with sequence and structural comparisons, suggests that the C-terminal 11 residues of EBP50 binds as an α-helix at the same site occupied in the dormant monomer by the last 11 residues of the inhibitory moesin C-terminal tail. Biochemical support for this interpretation derives from in vitro studies showing that appropriate mutations in both the EBP50 tail peptide and the FERM domain reduce binding, and that a peptide representing just the C-terminal 14 residues of EBP50 also binds to moesin. Combined with the recent identification of the I-CAM-2 binding site on the ERM FERM domain (Hamada, K., Shimizu, T., Yonemura, S., Tsukita, S., and Hakoshima, T. (2003) *EMBO J.* 22, 502-514), this study reveals that the FERM domain contains two distinct binding sites for membrane-associated proteins. The contribution of each ligand to ERM function can now be dissected by making structure-based mutations that specifically affect the binding of each ligand.

Key words: Moesin, Ezrin, EBP50, FERM

Introduction

The ezrin-radixin-moesin (ERM) family of closely related cytoskeletal proteins provide a regulated linkage between F-actin and membrane-associated proteins (Bretscher et al., 2002; Mangeat et al., 1999; Tsukita and Yonemura, 1999). The ERM proteins consist of an N-terminal ~300-residue FERM (four-point one ERM) domain, followed by a ~160-residue region predicted to be largely α-helical, and terminating in an ~90 residue C-terminal tail domain (Funayama et al., 1991; Gould et al., 1989; Lankes and Furthmayr, 1991; Pestonjamasp et al., 1995; Turunen et al., 1994). The ERM proteins exist in two states, a dormant state in which the FERM domain binds to its own C-terminal tail and thereby precludes binding of some partner proteins, and an activated state, in which the FERM domain binds to one of many membrane binding proteins and the C-terminal tail binds to F-actin. Phosphorylation of a threonine in the FERM domain (T235) and/or a threonine in the C-terminal region (T558 in moesin) and/or interactions with phosphatidylinositol (4,5)-bisphosphate [PtdIns(4,5)P_2] (Barret et al., 2000; Hayashi et al., 1999; Hirao et al., 1996; Matsui et al., 1998; Nakamura et al., 1999; Oshiro et al., 1998; Simons et al., 1998; Yang and Hinds, 2003; Yonemura et al., 2002) contribute to ERM protein activation. The cytoskeletal modulation achieved through the activities of the ERM proteins, and of the closely related tumor suppressor merlin, play important roles in cell signaling and growth control (Bretscher et al., 2002; Gusella et al., 1999).

The structure of the dormant moesin FERM:C-terminal tail complex (Pearson et al., 2000) showed that the FERM domain consists of three structural domains, designated lobes F1, F2 and F3, that together form a compact clover-shaped molecule (Fig. 1). Remarkably, the C-terminal tail binds the FERM domain in a highly extended structure consisting of one beta strand and four helical segments (αA-αD) spread over a large surface of lobes F2 and F3 (Fig. 1). While Pearson et al. (Pearson et al., 2000) identified six potential interaction sites on the FERM domain, it could not be predicted whether the masking of membrane protein binding sites was direct or indirect. Subsequently, the structures of the free active FERM domains of radixin (Hamada et al., 2000), moesin (Edwards and Keep, 2001) and ezrin (Smith et al., 2003) revealed that they differ from the dormant structure mostly by an increase in mobility and some large local conformational changes in lobes F2 and F3. Smith et al. (Smith et al., 2003) noted that the structural changes seemed most related to the loss of helices αA and αD of the C-terminal tail, and they predicted that these positions would be sites of tight binding of target proteins (Smith et al., 2003).

While the dormant and activated structures of the FERM domain are now well characterized, very little is known about how the FERM domain recognizes the many proteins with which it interacts. Membrane protein ligands for ERM proteins include the adhesion molecules CD44, CD43 and I-CAM-1, -2, -3 (Heiska et al., 1998; Helander et al., 1996; Serrador et al., 1997; Serrador et al., 1998; Serrador et al., 2002; Tsukita

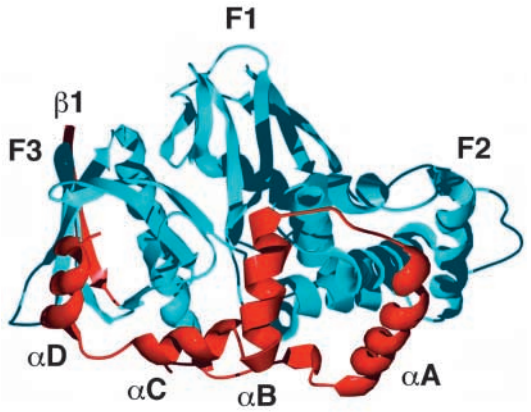

Fig. 1. The overall structure of dormant moesin. The N-terminal FERM domain (cyan) is associated with the C-terminal tail (red) which binds as an extended peptide inhibitor to block a large part of the surface of the FERM domain (from Pearson et al., 2000). The three FERM domain lobes are labeled as F1, F2 and F3 (F for FERM domain), and the major secondary structural elements of the C-terminal tail are labeled with the nomenclature used in this paper: β1 for the single β-strand, and αA, αB, αC and αD for the four α-helices. Fig. 1 was created with the programs Swiss-PdbViewer (Guex and Peitsch, 1997) and Pov-Ray (http://www.povray.org).

et al., 1994; Yonemura et al., 1998; Yonemura et al., 1993), and the two closely related scaffolding proteins EBP50/NHE-RF, the major ezrin binding protein in placenta, and NHE3 kinase A regulatory protein (E3KARP) (Reczek et al., 1997; Yun et al., 1998). The functional significance of differential binding to these various targets is not well understood, and the elucidation of how these various proteins are recognized will lay important groundwork for dissecting the complexities of ERM function.

The first determination of a membrane protein docking site came last year, with the structure of an I-CAM-2 peptide bound to the radixin FERM domain (Hamada et al., 2003). The peptide bound as a β-strand in the pocket that had been occupied by the β-strand of the C-terminal tail (see Fig. 1), and it was speculated that other adhesion molecules also bind at this site. Unfortunately, the data are unclear whether the ERM FERM:C-terminal tail interaction efficiently precludes binding of I-CAM-2 or other adhesion molecules (i.e. if the site is masked) (Heiska et al., 1998; Yonemura et al., 1998).

Here, we use crystallographic and biochemical analyses to analyze the binding of EBP50 to the active FERM domain. EBP50 and E3KARP have N-terminal PDZ domains that bind both membrane and cytoplasmic proteins (Bretscher et al., 2000; Bretscher et al., 2002; Weinman, 2001), and a C-terminal 30-residue region that provides a high affinity interaction with the ezrin and moesin FERM domains (Reczek and Bretscher, 1998). This binding site is completely masked in full-length dormant ezrin or moesin, or in a complex of the FERM domain with the C-terminal inhibitory tail (Reczek and Bretscher, 1998). We show that the C-terminal 11 residues of EBP50 provide a major component of the interaction with the FERM domain and act as a mimic of helix αD of the ERM C-terminal tail. Thus, the binding of EBP50 provides a clear example of a binding site that is directly masked in the dormant state of ERM proteins.

Materials and Methods

Peptide synthesis

Peptides P38 and P14 (Fig. 2C) were synthesized by the Cornell BioResource Center. The purity and mass of each peptide was confirmed using HPLC and mass spectrometry.

Protein purification and crystallization

The moesin FERM domain (residues 1-297) was expressed in *Escherichia coli*, purified as described previously (Reczek et al., 1997), and stored at 3 mg/ml, as determined using an ε_{280}=0.7 mM^{-1} cm^{-1}. For crystallization, a 100 mM stock of the peptide P38 (Fig. 2C) in 50% ethanol was mixed with the moesin FERM domain at a molar ratio of 1.5:1, and passed through a 0.2 μm filter. Crystallization screening was performed in hanging drops with a sparse matrix screen (Crystal Screens I and II, Hampton Research). Initial screens used drops of 2 μl of sample plus 1 μl of reservoir, and for optimization 4 μl drops of sample and 2 μl of buffer were used. The best crystals grew using a reservoir of 8-12% PEG 4000 in 100 mM Tris, pH 8.0-8.5 or 100 mM Hepes, pH 7.0-7.5. The largest crystals were approximately 0.15×0.15×0.25 mm^3, but were poorly reproducible and grew in clusters that required manual separation.

X-ray data collection and analysis

For data collection, crystals were briefly immersed in a series of artificial mother liquors containing 15% PEG 4000, 100 mM Tris pH 8.0 or Hepes pH 7.0 and glycerol concentrations of 0, 5, 10 and 15%, and were frozen in a cold N_2 stream. Data were collected at –150°C at the Cornell High Energy Synchrotron Source (CHESS; Ithaca, NY) and at the Advanced Light Source (ALS; Berkeley, CA), and processed with the programs Denzo/Scalepack (Otwinowski and Minor, 1997) or MOSFLM and SCALA (Collaborative Computational Project, 1984). Five data sets extending to between 4 and 3 Å resolution were collected at CHESS and ALS. The crystals showed ~1.5% variation in the a and c axis lengths, and difference maps revealed the data sets had variable peptide occupancy. The analyses presented here are all based on the single data set that appeared to have the highest peptide occupancy (Table 1).

Molecular replacement and refinement were done using CNS (Brunger et al., 1998), with the moesin FERM domain (Pearson et al., 2000) used as the search model. The rotation function using data from 15-4 Å resolution gave a unique solution 9.7 sigma above the mean, and the translation function solution gave a correlation coefficient of 0.4. With 10% of the data used for cross-validation, rigid body refinement (∞-3.5Å resolution) brought the R/R-free values from 45.1/42.8% to 43.1/41.4%. With one molecule in the asymmetric unit, the crystals are fairly loosely packed with a solvent content of 68% (V_M=3.84). Overall scaling revealed that the diffraction was highly anisotropic with B_{11}=–69 $Å^2$, B_{22}=38 $Å^2$, B_{33}=31 $Å^2$, B_{13}=–32 $Å^2$, and consistent with this, statistics indicate that reliable data only extend to ~4.5 Å in the h-direction and to 3.5 Å in the k- and l-directions (data not shown). Most attempts at individual atomic refinement caused R-free to rise, but by adjusting the weights a minimization was

Table 1. X-ray data collection statistics

Space group	C2
Unit cell (Å)	a=126.6, b=70.1, c=62.7, β=105.9
Resolution range (Å)	∞-3.5 (3.63-3.5)
Unique obs	6712 (664)
Completeness (%)	99 (100)
Multiplicity	3.7 (3.9)
R_{meas} (%)	8.4 (44)

Data collected at –150°C at Cornell High Energy Synchroton Source (CHESS) using λ=0.943 Å.

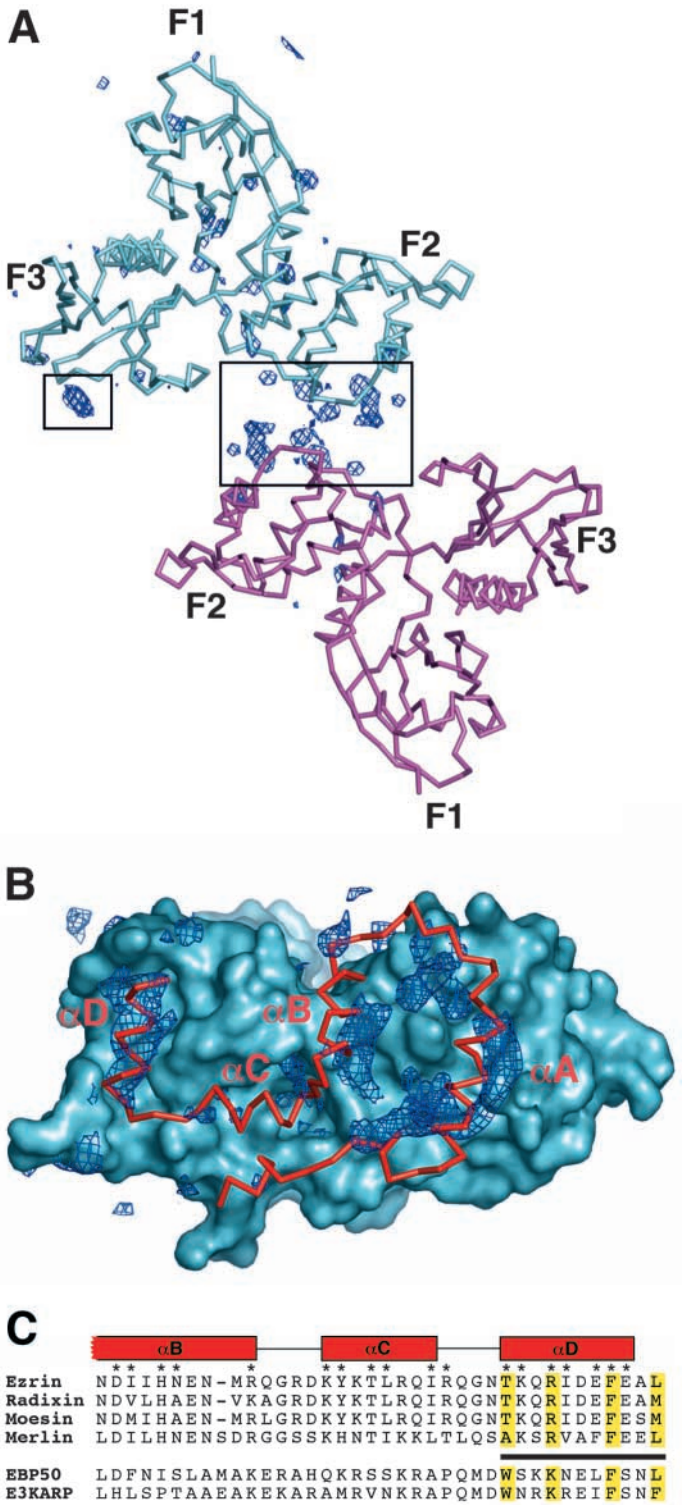

Fig. 2. Visualization of the binding of P38 to the FERM domain. (A) Final Fo-Fc electron density map, contoured at 3σ, of the P38: FERM complex (blue) shown with the Cα traces of two refined FERM domains (cyan and magenta) as they pack in the crystal. Boxes highlight the two major features of the difference map discussed in the text. The twofold crystallographic symmetry can be clearly seen in the density highlighted by the larger rectangle. A and B were prepared with the program PyMOL (DeLano, 2002). (B) View onto the F2-F3 face of the FERM domain (cyan surface) showing the same Fo-Fc electron density map contoured at 2 σ (blue). The C-terminal tail (rendered as a Cα backbone in red) is shown as it is seen bound in the dormant moesin structure (Pearson et al., 2000). (C) Alignment of the 38 C-terminal residues of EBP50 and E3KARP with the last 38 residues of the ERM proteins. Based on the dormant moesin complex, the secondary structures are drawn as a cartoon, and the residues buried at the interface with the FERM domain are marked with an asterisk. The eleven C-terminal residues that fit the difference density associated with the F3 lobe are indicated by a black bar, and the residues discussed in the text are highlighted in yellow.

carried out that yielded R/R-free=33.8/40.1%. For higher resolution refinements, an R-free of 40% would imply serious problems with the model, but experience shows that convergence at an R-free of 40% is reasonable for refinement against data that extend only to about 3.5/4.5 Å resolution [see figure 4A of Brunger (Brunger, 1997)].

EBP50-peptide fusion protein expression

DNA encoding the 39 C-terminal residues of EBP50 was amplified by PCR and cloned using the TOPO cloning kit (Invitrogen). Mutant constructs were also generated from the PCR clones using the Quick Change mutagenesis kit (Stratagene). The two EBP50 mutants consisted of a deletion of the C-terminal L358 and a F355R point mutation. Sequences of all constructs were confirmed by DNA sequencing. Maltose-binding protein (MBP)-EBP50-tail fusion proteins were expressed using the pMAL-c2 expression plasmid (New England Biolabs) transformed into the protease-deficient *E. coli* strain ER2508.

Site-directed mutagenesis of the FERM domain

The ezrin FERM mutant was made by recovering the DNA encoding the mutated residues (N210F and T214A) from a full length ezrin mutant (D.C. and A.B., unpublished data) by digestion with *Kpn*I and *Hpa*I and ligating it into a similarly digested ezrin FERM (1-297) construct (see Reczek et al., 1997). The construct was transformed into BL21 for expression and the protein was purified according to the FERM domain purification scheme (Reczek et al., 1997), except that the cultures were grown at 29°C overnight following induction to increase the yield of soluble protein.

Binding experiments

Ezrin FERM (1-297) was coupled to cyanogen bromide-activated Sepharose 4B beads (Sigma) at 2 mg protein per ml of beads as described previously (Reczek et al., 1997). 50 ml cultures of LB were inoculated with the protease-deficient *E. coli* strain ER2508 carrying plasmids for the expression of the MBP-EBP50 tail constructs. The cultures were grown to A_{600} of 0.8 and induced for 3 hours at 37°C by the addition of 2 mM isopropyl β-D-thiogalactopyranoside (IPTG) (Sigma). Control cell lysates were treated identically except that they did not receive the inducer. Cells were harvested, resuspended in 10 ml of buffer A (20 mM Hepes, 100 mM NaCl, pH 7.5 plus a bacterial protease inhibitor cocktail; Sigma), broken by sonication, and lysates were recovered after centrifugation at 30,000 ***g*** for 12 minutes. 12.5 μl of beads with immobilized ezrin FERM were incubated for 1 hour at 4°C on a rotating wheel with 1 ml of each of the clarified lysates. The beads were then washed four times with 1 ml of buffer A. Bound material was eluted by the addition of 100 μl of SDS gel sample buffer and boiled for 2 minutes. 8 μl of the recovered sample was resolved on a 10% SDS-PAGE gel followed by staining with Coomassie Brilliant Blue.

To evaluate the ability of the ezrin FERM domain to bind the C-terminal region of EBP50, P14 peptide (at 2 mg/ml) was covalently bound via its N-terminal Cys residue to SulfoLink Coupling Gel

(Pierce Biotechnology, Rockford, IL) according to the manufacturer's protocol. The peptide beads were then blocked with L-cysteine HCl, washed and stored in PBS plus 0.05% sodium azide as a 50% slurry. The same protocol without the peptide was followed to prepare control beads. For each binding experiment, 25 μl of a 50% bead slurry was washed twice with buffer A. 40 μg of ezrin FERM or ezrin mutant FERM in 400 μl buffer A was added to yield an estimated 10:1 molar ratio of bound peptide to protein. Tubes were rotated for 1 hour at room temperature, the beads were then collected and washed three times with 1 ml buffer A. Bound protein was eluted with successive treatments of 20 μl SDS sample buffer and boiling for 2 minutes. The two eluted fractions were combined and analyzed by SDS-PAGE.

Results

Crystallographic analysis of the peptide:FERM domain complex

To explore how EBP50 binds to the moesin FERM domain, a synthetic peptide (P38) corresponding to the last 38 amino acids of EBP50, plus an additional cysteinyl residue at the N terminus, was synthesized and co-crystallized with purified moesin FERM domain (residues 1-297). Crystals of the complex grew under conditions that did not lead to crystals in the absence of peptide. The crystals had highly anisotropic diffraction, but the structure could be solved by molecular replacement at a nominal resolution of 3.5 Å (see Materials and Methods). A difference electron density map showed two regions of strong difference density associated with lobes F2 and F3 indicating the putative peptide binding site(s) (Fig. 2A). Crystallographic refinement at this resolution is not very powerful (see Materials and Methods) and can be complicated by heavy model bias. For this reason, we have not refined a peptide model, but instead have worked to infer as much as possible from the unbiased difference electron density maps.

The difference electron density map revealed two features, whose interpretation was aided by comparison with the structure of the bound ERM C-terminal tail (Fig. 2B). The strongest electron density feature matches the position of αD of the C-terminal tail, and the shape of the density corresponds to about three turns of the helix. The second electron density feature is near a crystallographic twofold axis, making it appear more complex (Fig. 2A), but the unique density closest to the relevant FERM domain is close to the position of αA (Fig. 2B). At this resolution, the two electron density features do not have sufficient detail to assign them to specific residues of peptide P38. However, in the first case, we have been able to partly do this by noting that an important component of αD recognition in the dormant moesin complex is the α-carboxylate group of its C-terminal residue (Pearson et al., 2000; Smith et al., 2003), which is nestled into the FERM domain and bound by Asn210, Lys212, and Ser214. Assuming that P38 recognition at this site also involves an α-carboxylate group, then the residues bound must be the C-terminal ~11 residues of P38 (and EBP50). Remarkably, aligning the C-terminal sequence of ERM proteins with that of EBP50 and E3KARP revealed a heretofore overlooked similarity in sequence that makes this hypothesis quite plausible (Fig. 2C). In particular, this alignment shows conservation of hydrophobic residues at the two key buried positions of Phe574 and Met577 of moesin. Importantly, both residues are also conserved as hydrophobic in the equivalent segment of E3KARP. In addition, this alignment shows that Lys251 of EBP50 (and K330 of E3KARP) could duplicate the H-bond made by Arg570 of the moesin COOH-terminal ERM-association domain (C-ERMAD) with Glu244 on the FERM domain. Of additional note is the Trp348 side chain that is conserved between EBP50 and E3KARP. The ERM proteins have a Thr at the equivalent position (Fig. 2C), which is buried in the dormant moesin complex, so that a Trp substitution would seem unfavorable. However, when a Trp side chain is modeled into this position, it fits into a pocket surrounded by Phe240, Ile245, Ile257, Pro259, Ala264 and Phe267. We have insufficient clues to confidently interpret the second region of density associated with lobe F2 (see Discussion).

14 residues of EBP50 are sufficient for recognition

The first biochemical approach to validate our interpretation was to test the binding of a shorter EBP50 peptide. Since the electron density indicated the key involvement of at least 11 C-terminal residues of P38, we added three additional residues to avoid steric effects and synthesized P14, a peptide having the last 14 residues of EBP50 plus an additional Cys residue at the N terminus. The P14 peptide, covalently coupled to agarose beads, bound the wild-type ezrin FERM domain, whereas control beads lacking the peptide did not (Fig. 3A). Thus the 14 residues at the C terminus of EBP50 are sufficient for binding to the FERM domain.

Designed mutations of EBP50 and ezrin disrupt recognition

A second biochemical approach to validate our structural model was to test the effects of mutations in both EBP50 and ezrin specifically designed to disrupt the proposed interaction between the last 11 residues and F3 in the FERM domain. The EBP50 mutations were created in the context of a fusion between the maltose binding protein (MBP) and the 39 C-terminal residues of EBP50. The mutations of EBP50 targeted the two conserved hydrophobic residues, Phe355 and Leu358, that we propose are bound in complementary hydrophobic pockets in the FERM domain. The variants created were F355R, in which an arginine was substituted for Phe355, and L358Δ, in which (the C-terminal) Leu358 was deleted. Binding experiments showed that the mutations did disrupt binding: the fusion protein with wild-type EBP50 sequence was efficiently retained from a bacterial lysate by beads containing immobilized FERM domain, whereas the construct with F355R was not, and the construct with L358Δ was only poorly retained (Fig. 3B).

For testing the impact of mutations in the FERM domain, we used an N210F and T214A (N210F/T214A) double mutant of the ezrin FERM domain (originally created for another purpose; D.C. and A.B., unpublished data). As noted above, moesin residues Asn210 and Ser214 (Thr214 in ezrin) hydrogen-bond with the terminal α-carboxylate of the bound helix. In addition, Asn210 hydrogen-bonds to another carbonyl oxygen of the bound helix and stabilizes the functional conformation of the 210-214 turn in the FERM domain by hydrogen-bonding to the peptide nitrogen of residue 214. Consistent with our model for EBP50 recognition, the mutant ezrin FERM domain failed to be retained by beads on which P14 was immobilized (Fig. 3B).

Discussion

Taken together, the crystallographic data, the sequence

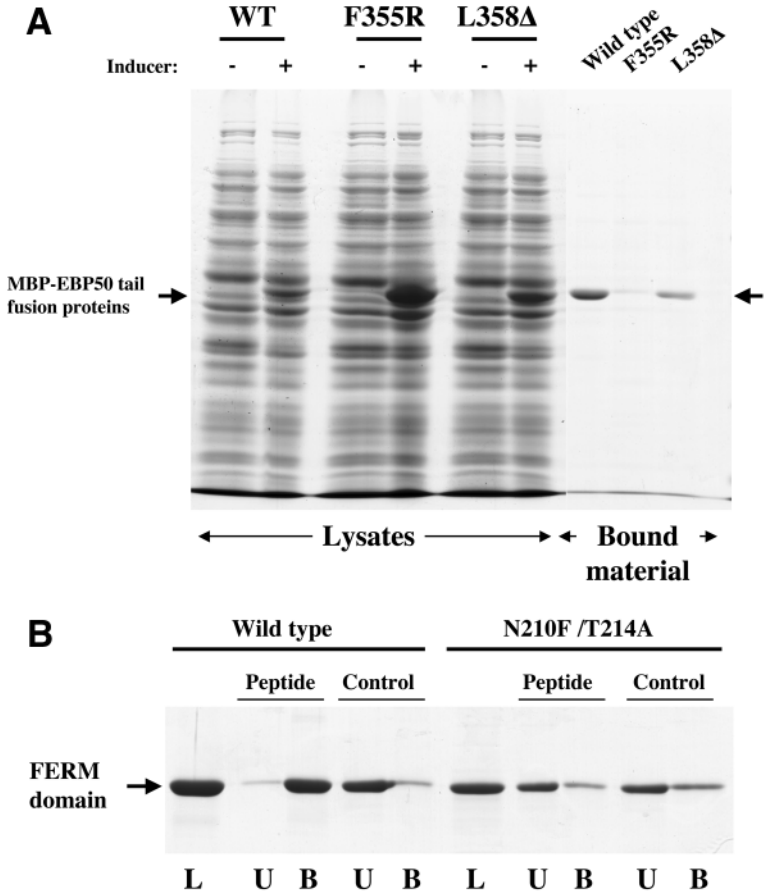

Fig. 3. Biochemical support that the C-terminal residues of EBP50 bind as proposed. (A) Residues F355 and L358 in the EBP50 tail are important for the interaction with the FERM domain. Bacteria containing plasmids for the expression of MBP fused to the C-terminal 39 residues of EBP50 (WT), or containing the F355R mutation (F355R) or the last residue deleted (L358Δ), were grown to log phase and either subjected to induced protein expression with IPTG (+) or not induced (–). Lysates were prepared and applied to beads on which the ezrin FERM domain had been immobilized. After washing, bound proteins were eluted and analyzed. The three eluates show proteins recovered from the induced lysates; essentially no material was recovered from parallel uninduced lysates (not shown). (B) The C-terminal 14 residue peptide of EBP50 binds to the FERM domain. Purified wild-type ezrin FERM domain (Wild type) or purified ezrin mutant N210F/T214A FERM domain (N210F/T214A) was mixed with beads containing covalently linked peptide (Peptide) or beads lacking the peptide (Control). The load (L), unbound (U), and bound and eluted (B) fractions were analyzed by SDS-PAGE.

similarity between the EBP50 and ERM tails and the binding properties of the two EBP50 mutants and the one ezrin mutant provide a compelling case for how the C-terminal 11 residues of EBP50 are recognized and bound by the FERM domain of ERM proteins. The salient feature is that the last ~11 residues of EBP50 bind to the FERM domain in such a way as to mimic the αD/lobeF3 interaction seen in dormant moesin. This provides a structural basis for the observed masking of the EBP50 binding site in dormant ERM proteins (Reczek and Bretscher, 1998).

In their analysis of the crystal structure of the free ezrin FERM domain, Smith et al. (Smith et al., 2003) introduced the concept of a 'keystone' interaction. Keystone interactions were defined as the contribution of residues from one protein or protein domain that allow another protein (or domain) to complete its fold. Because these interacting residues become an integral part of a protein's fold, they would most likely rarely dissociate and would be well suited to constructing macromolecular cytoskeletal complexes. In their analysis, they showed that αA and αD contribute keystone interactions for the F2 and F3 lobes, respectively. Smith et al. went on to predict that the binding sites for helices αA and αD could serve as high-affinity binding sites for other ligands that could duplicate or mimic this keystone function. The data show that EBP50 binds at the αD site and may be such a keystone mimic.

At this point, the interpretation and significance of the additional strong electron density associated with lobe F2 is unclear. It may indicate that other parts of the last 38 residues of EBP50 contribute to recognition, or because these difference map features are sandwiched between two molecules at a crystal contact, it is also possible that their binding is an artifact of crystallization. More structural and biochemical work will be required to sort this out. Nevertheless, it is clear that the C-terminal ~14 residues alone provide much of the binding specificity.

While we do not yet have a high resolution view of the moesin-EBP50 interaction, this work has revealed much valuable information. First is documentation of the unrecognized similarity between EBP50 and the ERM C-terminal tails, second is the concrete model for how the last 11 residues of EBP50 bind to ERM proteins, third is the documentation that the masking of the EBP50 binding site in dormant ERM proteins is the result of direct rather than indirect masking, and fourth is that the binding of EBP50 involves at least one of the keystone interaction sites identified by Smith et al. (Smith et al., 2003). Further insight into EBP50 recognition may be forthcoming from crystals of the radixin FERM domain complexed with a shorter EBP50 peptide (Terawaki et al., 2003). Importantly, the knowledge that EBP50 (and its relatives) binds to a different site on the FERM domain than does ICAM-2 (and related adhesion molecules) (Hamada et al., 2003) suggests that the FERM domain might be able to bind both classes of molecules simultaneously. This provides the first evidence that an ERM FERM domain may bind to two membrane-associated ligands simultaneously, and should allow the development of mutants that selectively disrupt one or the other function, paving the way for experiments that dissect which proteins are involved in which functions of ERM proteins.

We thank the MacCHESS staff for their help and suggestions during X-ray data collection and processing, and we thank W. L. DeLano for providing superb technical support for PyMOL. This work is based upon research conducted at the Cornell High Energy Synchroton Source (CHESS), which is supported by the National Science Foundation and NIGMS, National Institutes of Health Award DMR 9713424.

The atomic coordinates and structure factors (code 1SGH) have been deposited in the Protein Data Bank, Research Collabatory for Structural Bioinformatics, Rutgers University, New Brunswick, NJ (http://www.rcsb.org/).

References

Barret, C., Roy, C., Montcourrier, P., Mangeat, P. and Niggli, V. (2000). Mutagenesis of the phosphatidylinositol 4,5-bisphosphate (PIP(2)) binding site in the NH(2)-terminal domain of ezrin correlates with its altered cellular distribution. *J. Cell Biol.* **151**, 1067-1080.

Bretscher, A., Chamber, C., Nguyen, R. and Reczek, D. (2000). ERM-merlin and EBP50 protein families in plasma membrane organization and function. *Annu. Rev. Cell Dev. Biol.* **16**, 113-143.

Bretscher, A., Edwards, K. and Fehon, R. G. (2002). ERM proteins and merlin: integrators at the cell cortex. *Nat. Rev. Mol. Cell. Biol.* **3**, 586-599.

Brunger, A. T. (1997). Free R value: cross-validation in crystallography. *Methods Enzymol.* **277**, 366-396.

Brunger, A. T., Adams, P. D., Clore, G. M., DeLano, W. L., Gros, P., Grosse-Kunstleve, R. W., Jiang, J. S., Kuszewski, J., Nilges, M., Pannu, N. S. et al. (1998). Crystallography & NMR system: A new software suite for macromolecular structure determination. *Acta Crystallogr. D. Biol. Crystallogr.* **54**, 905-921.

Collaborative Computational Project (1984). The CCP4 suite: programs for protein crystallography. *Acta Crystallogr. D. Biol. Crystallogr.* **50**, 760-763.

DeLano, W. L. (2002). *The PyMOL Molecular Graphics System*. San Carlos, CA, USA: DeLano Scientific.

Edwards, S. D. and Keep, N. H. (2001). The 2.7 A crystal structure of the activated FERM domain of moesin: an analysis of structural changes on activation. *Biochemistry (Mosc.)* **40**, 7061-7068.

Funayama, N., Nagafuchi, A., Sato, N., Tsukita, S. and Tsukita, S. (1991). Radixin is a novel member of the band 4.1 family. *J. Cell Biol.* **115**, 1039-1048.

Gould, K. L., Bretscher, A., Esch, F. S. and Hunter, T. (1989). cDNA cloning and sequencing of the protein-tyrosine kinase substrate, ezrin, reveals homology to band 4.1. *EMBO J.* **8**, 4133-4142.

Guex, N. and Peitsch, M. C. (1997). SWISS-MODEL and the Swiss-PDBViewer: An environment for comparative protein modeling. *Electrophoresis* **18**, 2714-2723.

Gusella, J. F., Ramesh, V., MacCollin, M. and Jacoby, L. B. (1999). Merlin: the neurofibromatosis 2 tumor suppressor. *Biochim. Biophys. Acta* **1423**, M29-M36.

Hamada, K., Shimizu, T., Matsui, T., Tsukita, S. and Hakoshima, T. (2000). Structural basis of the membrane-targeting and unmasking mechanisms of the radixin FERM domain. *EMBO J.* **19**, 4449-4462.

Hamada, K., Shimizu, T., Yonemura, S., Tsukita, S. and Hakoshima, T. (2003). Structural basis of adhesion-molecule recognition by ERM proteins revealed by the crystal structure of the radixin-ICAM-2 complex. *EMBO J.* **22**, 502-514.

Hayashi, K., Yonemura, S., Matsui, T., Tsukita, S. and Tsukita, S. (1999). Immunofluorescence detection of ezrin/radixin/moesin (ERM) proteins with their carboxyl-terminal threonine phosphorylated in cultured cells and tissues. *J. Cell Sci.* **112**, 1149-1158.

Heiska, L., Alfthan, K., Gronholm, M., Vilja, P., Vaheri, A. and Carpen, O. (1998). Association of ezrin with intercellular adhesion molecule-1 and -2 (ICAM-1 and ICAM-2). Regulation by phosphatidylinositol 4, 5-bisphosphate. *J. Biol. Chem.* **273**, 21893-21900.

Helander, T. S., Carpen, O., Turunen, O., Kovanen, P. E., Vaheri, A. and Timonen, T. (1996). ICAM-2 redistributed by ezrin as a target for killer cells. *Nature* **382**, 265-268.

Hirao, M., Sato, N., Kondo, T., Yonemura, S., Monden, M., Sasaki, T., Takai, Y., Tsukita, S. and Tsukita, S. (1996). Regulation mechanism of ERM (ezrin/radixin/moesin) protein/plasma membrane association: possible involvement of phosphatidylinositol turnover and Rho-dependent signaling pathway. *J. Cell Biol.* **135**, 37-51.

Lankes, W. T. and Furthmayr, H. (1991). Moesin: a member of the protein 4.1-talin-ezrin family of proteins. *Proc. Natl. Acad. Sci. USA* **88**, 8297-8301.

Mangeat, P., Roy, C. and Martin, M. (1999). ERM proteins in cell adhesion and membrane dynamics. *Trends Cell Biol.* **9**, 187-192.

Matsui, T., Maeda, M., Doi, Y., Yonemura, S., Amano, M., Kaibuchi, K., Tsukita, S. and Tsukita, S. (1998). Rho-kinase phosphorylates COOH-terminal threonines of ezrin/radixin/moesin (ERM) proteins and regulates their head-to-tail association. *J. Cell Biol.* **140**, 647-657.

Nakamura, F., Huang, L., Pestonjamasp, K., Luna, E. J. and Furthmayr, H. (1999). Regulation of F-actin binding to platelet moesin In vitro by both phosphorylation of threonine 558 and polyphosphatidylinositides. *Mol. Biol. Cell* **10**, 2669-2685.

Oshiro, N., Fukata, Y. and Kaibuchi, K. (1998). Phosphorylation of moesin by rho-associated kinase (Rho-kinase) plays a crucial role in the formation of microvilli-like structures. *J. Biol. Chem.* **273**, 34663-34666.

Otwinowski, Z. and Minor, W. (1997). Processing of X-ray diffraction data collected in oscillation mode. In *Methods Enzymol.* vol. 276: Macromolecular Crystallography, part A (eds J. Carter, C. W. and R. M. Sweet), pp. 307-326. New York: Academic Press.

Pearson, M., Reczek, D., Bretscher, A. and Karplus, P. (2000). Structure of the ERM protein moesin reveals the FERM domain fold masked by an extended actin binding tail domain. *Cell* **101**, 259-270.

Pestonjamasp, K., Amieva, M. R., Strassel, C. P., Nauseef, W. M., Furthmayr, H. and Luna, E. J. (1995). Moesin, ezrin, and p205 are actin-binding proteins associated with neutrophil plasma membranes. *Mol. Biol. Cell* **6**, 247-259.

Reczek, D., Berryman, M. and Bretscher, A. (1997). Identification of EBP50: A PDZ-containing phosphoprotein that associates with members of the ezrin-radixin-moesin family. *J. Cell Biol.* **139**, 169-179.

Reczek, D. and Bretscher, A. (1998). The carboxyl-terminal region of EBP50 binds to a site in the amino- terminal domain of ezrin that is masked in the dormant molecule. *J. Biol. Chem.* **273**, 18452-18458.

Serrador, J. M., Alonso-Lebrero, J. L., del Pozo, M. A., Furthmayr, H., Schwartz-Albiez, R., Calvo, J., Lozano, F. and Sanchez-Madrid, F. (1997). Moesin interacts with the cytoplasmic region of intercellular adhesion molecule-3 and is redistributed to the uropod of T lymphocytes during cell polarization. *J. Cell Biol.* **138**, 1409-1423.

Serrador, J. M., Nieto, M., Alonso-Lebrero, J. L., del Pozo, M. A., Calvo, J., Furthmayr, H., Schwartz-Albiez, R., Lozano, F., Gonzalez-Amaro, R., Sanchez-Mateos, P. et al. (1998). CD43 interacts with moesin and ezrin and regulates its redistribution to the uropods of T lymphocytes at the cell-cell contacts. *Blood* **91**, 4632-4644.

Serrador, J. M., Vicente-Manzanares, M., Calvo, J., Barreiro, O., Montoya, M. C., Schwartz-Albiez, R., Furthmayr, H., Lozano, F. and Sanchez-Madrid, F. (2002). A novel serine-rich motif in the intercellular adhesion molecule 3 is critical for its ezrin/radixin/moesin-directed subcellular targeting. *J. Biol. Chem.* **277**, 10400-10409.

Simons, P. C., Pietromonaco, S. F., Reczek, D., Bretscher, A. and Elias, L. (1998). C-terminal threonine phosphorylation activates ERM proteins to link the cell's cortical lipid bilayer to the cytoskeleton. *Biochem. Biophys. Res. Commun.* **253**, 561-565.

Smith, W. J., Nassar, N., Bretscher, A., Cerione, R. A. and Karplus, P. A. (2003). Structure of the active N-terminal domain of Ezrin. Conformational and mobility changes identify keystone interactions. *J. Biol. Chem.* **278**, 4949-4956.

Terawaki, S. I., Maesaki, R., Okada, K. and Hakoshima, T. (2003). Crystallographic characterization of the radixin FERM domain bound to the C-terminal region of the human Na+/H+-exchanger regulatory factor (NHERF). *Acta Crystallogr. D. Biol. Crystallogr.* **59**, 177-179.

Tsukita, S., Oishi, K., Sato, N., Sagara, J., Kawai, A. and Tsukita, S. (1994). ERM family members as molecular linkers between the cell surface glycoprotein CD44 and actin-based cytoskeletons. *J. Cell Biol.* **126**, 391-401.

Tsukita, S. and Yonemura, S. (1999). Cortical actin organization: lessons from ERM (Ezrin/Radixin/Moesin) proteins. *J. Biol. Chem.* **274**, 34507-34510.

Turunen, O., Wahlstrom, T. and Vaheri, A. (1994). Ezrin has a COOH-terminal actin-binding site that is conserved in the ezrin protein family. *J. Cell Biol.* **126**, 1445-1453.

Weinman, E. J. (2001). New functions for the NHERF family of proteins. *J. Clin. Invest.* **108**, 185-186.

Yang, H. S. and Hinds, P. W. (2003). Increased ezrin expression and activation by CDK5 coincident with acquisition of the senescent phenotype. *Mol. Cell* **11**, 1163-1176.

Yonemura, S., Hirao, M., Doi, Y., Takahashi, N., Kondo, T., Tsukita, S. and Tsukita, S. (1998). Ezrin/radixin/moesin (ERM) proteins bind to a positively charged amino acid cluster in the juxta-membrane cytoplasmic domain of CD44, CD43, and ICAM-2. *J. Cell Biol.* **140**, 885-895.

Yonemura, S., Matsui, T. and Tsukita, S. (2002). Rho-dependent and -independent activation mechanisms of ezrin/radixin/moesin proteins: an essential role for polyphosphoinositides in vivo. *J. Cell Sci.* **115**, 2569-2580.

Yonemura, S., Nagafuchi, A., Sato, N. and Tsukita, S. (1993). Concentration of an integral membrane protein, CD43 (leukosialin, sialophorin), in the cleavage furrow through the interaction of its cytoplasmic domain with actin-based cytoskeletons. *J. Cell Biol.* **120**, 437-449.

Yun, C. H., Lamprecht, G., Forster, D. V. and Sidor, A. (1998). NHE3 kinase A regulatory protein E3KARP binds the epithelial brush border Na+/H+ exchanger NHE3 and the cytoskeletal protein ezrin. *J. Biol. Chem.* **273**, 25856-25863.